



Rainfall-Riverflow Trends of Enyong Creek in Akwa Ibom State, Nigeria

¹AUGUSTINE, CU; ²AHANEKU, IE; ³AWU, JI

¹Ministry of Agriculture, Uyo Akwa Ibom State, Nigeria

²Michael Okpara University of Agriculture Umudike, Abia State, Nigeria

³National Centre for Agricultural Mechanization, Ilorin, Kwara State, Nigeria

*Corresponding Email Address: ecoagricultural@gmail.com

Co-Authors Email: alleybury@yahoo.com; drahaneku@yahoo.com; ecoagricultural@gmail.com

ABSTRACT: Rainfall-riverflow is crucial for effective hydrology and water resource management. Hence, the objective of this study was to evaluate the rainfall-riverflow trends of Enyong Creek in Akwa Ibom State, Nigeria, utilizing daily hydro-meteorological data of daily rainfall, river discharge, and temperature data collected from the period 2018 to 2023 and modeling the data by Vector Autoregressive (VAR) models. The results show that the VAR model successfully captured the dynamic relationships among water discharge (WD), rainfall (RF), and average temperature (AVE.TEMP). Equations revealed the influence of past values on the current state of each variable. Correlation matrix and graphical representations confirmed model adequacy. Validation results demonstrated the model's accuracy, with model R-squared value of 0.8781 indicating a strong correlation. The performance measurement of evaluation for the developed model showed a Mean Average Error (MAE), Root Mean Square error (RMSE), and Mean Absolute Percentage Error (MAPE) values of 5.5066, 6.7831, and 7.4203 respectively, revealing a satisfactory accuracy and precision. Information derived from this study offers valuable insights for government officials, policymakers, and planners in accurate flood forecasting, emergency management, land use planning, and infrastructure development

DOI: <https://dx.doi.org/10.4314/jasem.v28i1.4>

Open Access Policy: All articles published by **JASEM** are open-access articles under **PKP** powered by **AJOL**. The articles are made immediately available worldwide after publication. No special permission is required to reuse all or part of the article published by **JASEM**, including plates, figures and tables.

Copyright Policy: © 2024 by the Authors. This article is an open-access article distributed under the terms and conditions of the **Creative Commons Attribution 4.0 International (CC-BY- 4.0)** license. Any part of the article may be reused without permission provided that the original article is cited.

Cite this paper as: AUGUSTINE, C. U; AHANEKU, I. E; AWU, J. I. (2023). Rainfall-Riverflow Trends of Enyong Creek in Akwa Ibom State, Nigeria. *J. Appl. Sci. Environ. Manage.* 28 (1) 27-35

Dates: Received: 10 December 2023; Revised: 11 January 2024; Accepted: 21 January 2024 Published: 30 January 2024

Keywords: Rainfall-Riverflow Trends, Vector Autoregressive, River Discharge, Flood Forecasting

Stochastic modeling of rainfall-riverflow plays a pivotal role in hydrology and the management of water resources. The stochastic rainfall-river flow modeling involves the use of probabilistic and statistical methods to simulate the variability and uncertainty of rainfall and river flow patterns (Ahaneku and Otache, 2014). This methodology utilizes probabilistic and statistical approaches to model the variability and uncertainty inherent in rainfall-riverflow patterns. The significance of stochastic rainfall-riverflow modeling is underscored by its contributions to various aspects, including comprehending hydrological processes, managing floods and droughts, optimizing reservoir operations and water allocation, designing infrastructure, adapting to climate change, conducting risk assessments, facilitating hydropower generation,

ensuring environmental protection, addressing data-scarce regions, and supporting research and education. Flood forecasting system integrating meteorology, hydrology, technology, and communication, is instrumental in issuing early warnings to mitigate the impacts of flooding. This field continuously advances alongside developments in science and technology, aiming to enhance the protection of people and property against the consequences of this natural disaster, flood (WMO, 2023). Floods, recognized as one of the most recurring and devastating natural hazards, profoundly affect human lives and result in substantial economic losses globally (Khan *et al.*, 2011). It is acknowledged that the risks associated with flooding will persist in the future, exacerbated by climate change leading to increased intensity and

*Corresponding Email Address: ecoagricultural@gmail.com

frequency of floods in various regions worldwide (Jonkman and Dawson, 2012). Flood occurrences are primarily driven by the rapid accumulation and release of runoff waters, triggered by intense rainfall. The swift rise to peak discharge and subsequent rapid decline characterize these events. The prevalence of flooding is a significant concern in hydrological and natural hazards science, ranking high among natural disasters in terms of both global population impact and individual fatalities (Borga *et al.*, 2014). The potential for flood-related casualties and damages is further increasing in numerous regions due to ongoing social and economic development, exerting pressure on land-use, particularly through urbanization. The frequency and severity of flood vulnerability are anticipated to escalate due to the impacts of global climate change, characterized by intense weather events such as heavy rainfall and river discharge conditions (Dihn *et al.*, 2014). Addressing the current trajectory and potential future scenarios of flood risks necessitates accurate spatial and temporal information on potential hazards and risks associated with floods. As reported by Chang and Guo (2006), heavy convective rainfall often results in flooding in urban areas. The conversion of agricultural land, depletion of natural vegetation, and population growth in flood-prone areas exacerbate this risk, disrupting natural infiltration processes. The consequences of flooding vary across regions, with Nigeria experiencing its share of flood events resulting in significant losses of lives and property. In Nigeria, the various factors contributing to flooding, including the accumulation of refuse leading to blockages in natural waterways, high-intensity rainfall on gentle slopes, dam failures, and rapid unplanned settlement affecting drainage systems. While complete eradication of floods may be impractical, minimizing their impact is feasible through a holistic understanding of contributing factors. Implementing an early warning system becomes crucial for effective risk assessment in spatial planning, facilitating resource allocation for emergency response teams and infrastructure protection. Forecasting plays a fundamental role in flood management, guiding decisions related to closing flood gates, activating protective measures, and enabling communities to prepare for potential flooding through evacuations and resource provisioning. The components of flood forecasting systems encompass data collection, involving monitoring weather conditions, river levels, snowpack, and soil moisture. Mathematical and computational models predict how changes in these variables impact river discharge and water levels. Warning systems, automated to issue alerts to emergency management agencies and the public, and effective communication of forecasts are critical elements in minimizing flood-related risks and

protecting human life, property, and natural ecosystems.

However, Flood forecasting encompasses various types of floods, such as riverine floods, flash floods, coastal floods, and urban floods, each requiring tailored forecasting methods based on the specific flood type and geographical location (Parker and Wilby, 2005). Technological advancements over the years have significantly enhanced the precision and timeliness of flood forecasting, utilizing tools like weather radar, satellite imagery, remote sensing, and computer modeling to deliver more accurate predictions. As a multidisciplinary field integrating meteorology, hydrology, technology, and communication, flood forecasting aims to provide early warnings and mitigate the impacts of flooding (Merz *et al.*, 2020). It continually evolves with scientific and technological progress to enhance protection against this natural disaster. However, it is not without challenges, facing uncertainties in weather forecasts, the intricate nature of hydrological processes, the influence of urbanization on local drainage systems, and the necessity for effective communication to ensure public responsiveness. Public education and community involvement are integral aspects, contributing significantly to the effectiveness of the forecasting system when communities are well-informed about risks and have clear guidance on responding to warnings. Historical advancements in meteorology and hydrology from the late 19th to the early 20th century, including the utilization of precipitation data, laid the foundation for more comprehensive flood forecasting (Kidd and Huffman, 2011). The mid-20th century witnessed the introduction of numerical weather models, enhancing precipitation forecasting and understanding its potential impact on flooding. Concurrently, hydrological models, simulating water movement in river basins, emerged to improve forecasting accuracy. The 21st century has brought challenges from climate change, resulting in more frequent and intense rainfall events and altered flood patterns. In response, forecasting models and techniques are being updated to accommodate changing climate conditions (Alfieri and Pappenberger, 2019). Recent advancements in big data analytics and machine learning enable more sophisticated flood forecasting models capable of processing and analyzing vast amounts of data in real-time, thereby improving accuracy and lead time in flood predictions. Therefore, this objective of this study was to evaluate the rainfall-riverflow trends of Enyong Creek in Akwa Ibom State, Nigeria, utilizing hydro-meteorological data of daily rainfall, river discharge, and temperature data collected from the

period 2018 to 2023 and modeling the data by Vector Autoregressive (VAR) model.

MATERIALS AND METHODS

Study Area: The study area is situated between latitudes 5°11' to 5°28' N and longitudes 7°51'E, covering a geographic expanse of 55.63 km² (Figure 1). Geologically, the region displays a diverse range of formations, ranging from the Asu River Formations within the Abakiliki Anticlinorium to recent alluvium in the southern part. The Asu River Group predominantly underlies the northern section of the study area, featuring intense fracturing evident in outcrops like those in Uburu. The Albian-aged Asu River Group comprises three formations, characterized by bluish-grey to olive-brown shales, sandy shales, fine-grained micaceous and calcareous

sandstones, along with some limestones. The landscape is marked by structurally controlled ridges, denudational hills such as the 150m high Obotme conical hill, steep-sided valleys, and geographical features like saddles and cols at Obot Ito Ikpo. Extensive wetlands and alluvial plains contribute to soil covers consisting of silty clay, sandy areas, and heavily weathered loamy and alluvial deposits. The region experiences a tropical climate, with temperatures ranging from 26 to 32° C. Temperature fluctuations are relatively uniform, except during the dry months when temperature increases are more pronounced than during the extended wet period (March to October). The proximity to the main Cross River Channel results in high humidity levels (84%). The average annual rainfall in the basin measures 2200mm, with a significant contribution from southwest tropical maritime air-masses.

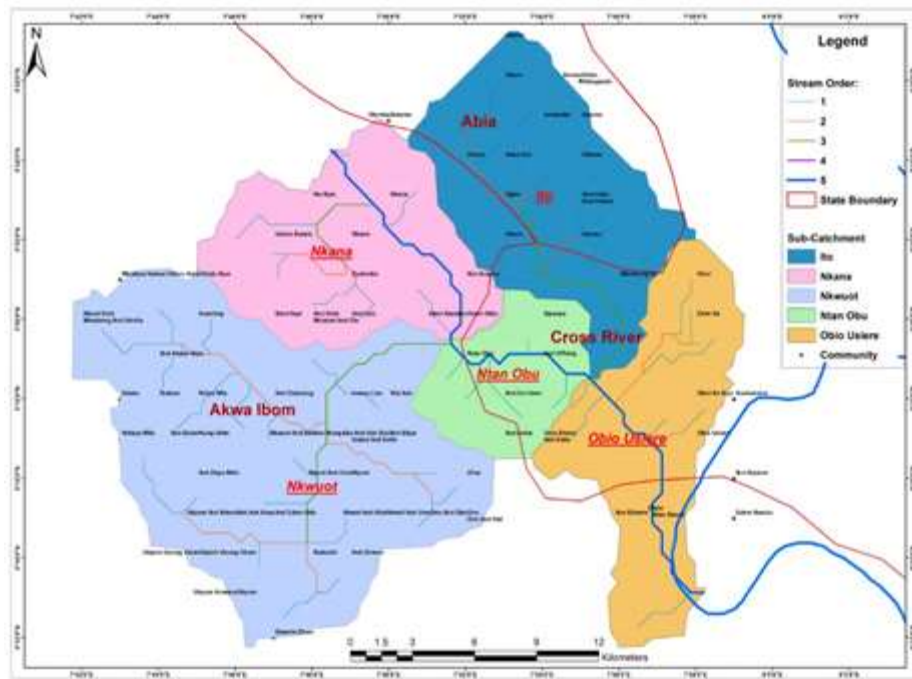


Fig. 1: Delineation Map of the Enyong Creek of Aka Ibom State, Nigeria

$$\begin{aligned}
 y_t &= \beta_{y0}\beta_{yy1}y_{t-1} + \dots + \beta_{yy p}y_{t-p} + \beta_{yx1}x_{t-1} + \dots + \beta_{yx p}x_{t-p} + v_t^y & 1 \\
 x_t &= \beta_{x0}\beta_{xy1}y_{t-1} + \dots + \beta_{xy p}y_{t-p} + \beta_{xx1}x_{t-1} + \dots + \beta_{xx p}x_{t-p} + v_t^x & 2
 \end{aligned}$$

Methods: The vector autoregressive (VAR) model is for the analysis of multivariate time series. A VAR system contains a set of *m* variables, each of which is expressed as a linear function of *p* lags of itself and of all of the other *m*-1 variable, plus an error term, *ε*. With two variables, *x* and *y*, an order-*p* VAR would be the two equations 1 and 2;

The model development process included:

Data Exploration: Visualization of the data was carried out to understand the patterns, trends, and seasonality present in each time series. Equally, the data summary statistics was calculated and identify any apparent correlations between the variables.

Data Stationarity: The VAR models assume that the data is stationary. Performing stationarity tests (e.g., Augmented Dickey-Fuller) for each time series to

check for non-stationarity was mandatory and it was carried out.

Model Order Selection: To determine the appropriate lag order for the VAR model. The use of information criteria like AIC, BIC, or Ljung-Box tests to select the lag order that best fits the data were employed.

Data Splitting: The dataset was divided into training and testing sets. The training set was used to estimate the VAR model, and the testing set for model evaluation.

VAR Model Estimation: I used Python libraries like Statsmodels to estimate the VAR model. For example, “python: from statsmodels.tsa.api import VAR
model = VAR(train_data)
model_fitted = model.fit(4)”

Forecasting: Using the fitted VAR model to make forecasts for water discharge, rainfall, and average temperature into the future.
“python:

forecast = model_fitted.forecast(model_fitted.y, steps=n_steps)”

Model Evaluation: Comparing the model's forecasts to the actual values in the testing set using appropriate evaluation metrics such as the Mean Average Error (MAE), Root Mean Square Error (RMSE), Mean Absolute Percentage Error (MAPE), and R-Squared (R2) were used to determine the performance of the models developed.

Interpretation: Analysing the VAR model's coefficient matrices to understand the causal relationships between the variables and their lagged effects was carried out.

Visualization: Visualization of the model's forecasts and comparing them to the observed data to assess the model's performance was also carried out. The structural block diagram of the Vector autoregressive model development is shown in Figure 2

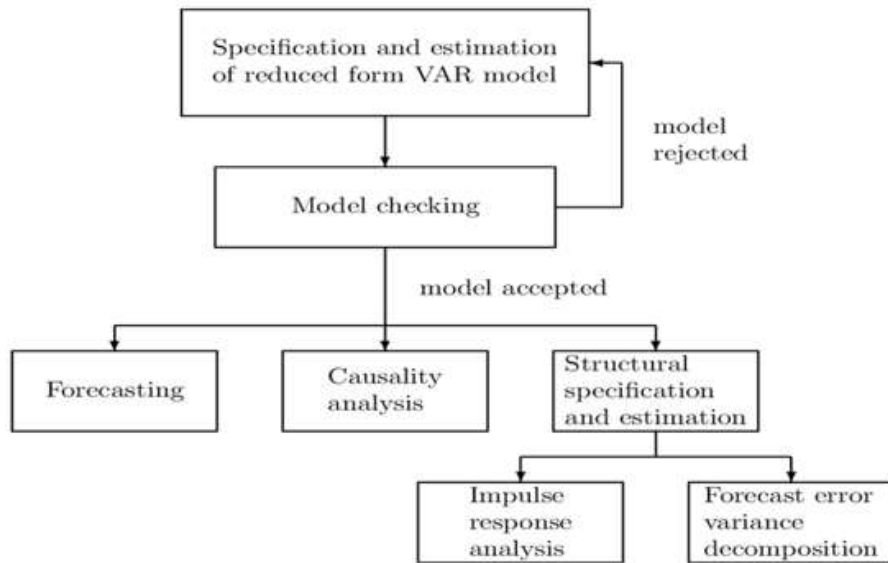


Fig 2: The structural Block Diagram of Vector Autoregressive Model Development (Source: Helmut Luetkepohl, 2007)

RESULTS AND DISCUSSION

The VAR model was modeled evaluated and compared on a number of different factors. The numerical and graphical assessment of their performance in terms of accuracy, reliability, and lead time for flood forecasting were determined. The descriptive graph representation of data visualizing to know whether the parameters (Water Discharge (WD), Rainfall (RF), and Average Temperature (AVE.TEMP)) data is stationary or non-stationary is shown in Figure 2 The data graph visualization for the Water Discharge(WD) is represented as blue color, rainfall Humidity(RH) is represented as orange color and Average Temperature (AVG_TEMP) is represented as green color.

From Figure 2, the dataset was subjected to the AD-fuller test, however, it was discovered that that AD Statistic of - 3.9194437722354185 was less than the three Critical Values: {'1%': - 3.4339700129534423, '5%': - 2.8631390341376393, '10%': - 2.567621272963846} and a p-value: 0.0018963213250938582 signifying it is a stationary time series data set. The VAR model

statistical summary for the three parameters used are given in Tables 1 to 4

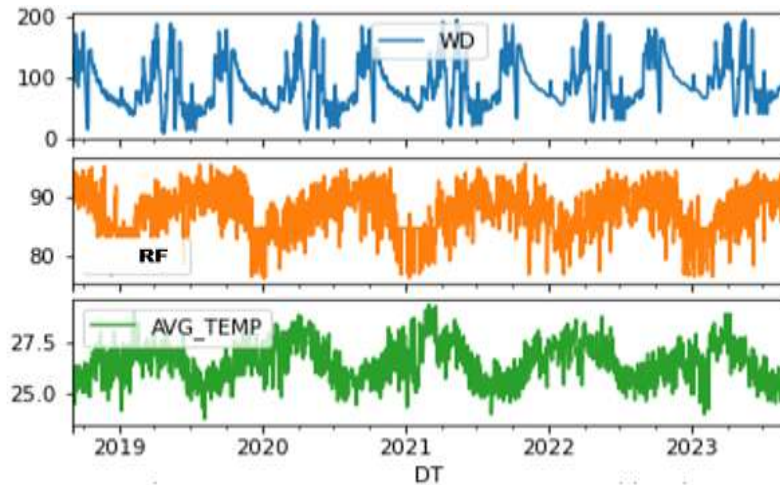


Fig 2: The structural Block Diagram of Vector Autoregressive Model Development

Table 1: The Statistical Summary of Regression Results

| Model: | VAR | | |
|-------------------|--------------------|------------------|---------|
| Method: | OLS | | |
| Date: | Fri, 20, Oct, 2023 | | |
| Time: | 11:25:14 | | |
| No. of Equations: | 3.00000 | BIC: | 6.69601 |
| Nobs: | 1791.00 | HQIC: | 6.62060 |
| Log likelihood: | -13474.2 | FPE: | 717.990 |
| AIC: | 6.57645 | Det (Omega_mle): | 702.579 |

Table 2: The Statistical Summary Results for Water Discharge (WD) equation

| | coefficient | std. error | t-stat | prob. |
|-------------|-------------|------------|--------|-------|
| Const. | -30.735576 | 25.522443 | -1.204 | 0.228 |
| L1.WD | 0.977359 | 0.023688 | 41.260 | 0.000 |
| L1.RF | -0.043293 | 0.165075 | -0.262 | 0.793 |
| L1.AVG_TEMP | -0.484993 | 0.748628 | -0.648 | 0.517 |
| L2.WD | -0.101073 | 0.033137 | -3.050 | 0.002 |
| L2.RF | 0.265705 | 0.179884 | 1.477 | 0.140 |
| L2.AVG_TEMP | 0.994903 | 0.884948 | 1.124 | 0.261 |
| L3.WD | 0.048196 | 0.033140 | 1.454 | 0.146 |
| L3.RF | 0.012498 | 0.179491 | 0.070 | 0.944 |
| L3.AVG_TEMP | -0.819405 | 0.886125 | -0.925 | 0.355 |
| L4.WD | -0.031498 | 0.023760 | -1.326 | 0.185 |
| L4.RF | 0.002013 | 0.157492 | 0.013 | 0.990 |
| L4.AVG_TEMP | 1.034040 | 0.751513 | 1.376 | 0.169 |

Table 3: Statistical Summary Results for equation RF

| | Coefficient | Std. Error | T-Stat | Prob. |
|-------------|-------------|------------|--------|-------|
| Const. | 15.357379 | 4.340417 | 3.538 | 0.000 |
| L1.WD | 0.002701 | 0.004028 | 0.670 | 0.503 |
| L1.RF | 0.483552 | 0.028073 | 17.225 | 0.000 |
| L1.AVG_TEMP | 1.146141 | 0.127314 | 9.002 | 0.000 |
| L2.WD | 0.004758 | 0.005635 | 0.844 | 0.398 |
| L2.RF | 0.050206 | 0.030591 | 1.641 | 0.101 |
| L2.AVG_TEMP | -0.436397 | 0.150497 | -2.900 | 0.004 |
| L3.WD | -0.007552 | 0.005636 | -1.340 | 0.180 |
| L3.RF | 0.161872 | 0.030525 | 5.303 | 0.000 |
| L3.AVG_TEMP | -0.040890 | 0.150697 | -0.271 | 0.786 |
| L4.WD | 0.001745 | 0.004041 | 0.432 | 0.666 |
| L4.RF | 0.100994 | 0.026784 | 3.771 | 0.000 |
| L4.AVG_TEMP | -0.581518 | 0.127804 | -4.550 | 0.000 |

The Vector Autoregressive (VAR) model statistical summary generated contains the results for a multivariate time series analysis involving three variables: WD (Water Discharge), RF (Rainfall), and AVG_TEMP (Average Temperature). The VAR models were used to understand the relationships and dependencies between the multiple time series variables. The Significance of number of equations the model specifies are of three equations, one for each variable WD, RF, and AVG_TEMP, respectively. Each equation represents how the current value of a variable depends on its own past values and the past values of the other variables. The BIC, HQIC, AIC information criteria are information criteria that was used for the model selection. The lower values indicate better model fit. In this case, the BIC, HQIC, and AIC values were used for selecting the lag order of the VAR model. Also, the log likelihood measures the goodness of fit of the model to the data. less negative values indicating better fit. However, the FPE (Final Prediction Error) is another measure of model adequacy. Smaller values indicate a better model fit. The VAR model equations developed is given in equations 3 to 5. The equations appear to be a set of simultaneous equations that represent a system of dynamic relationships between three variables: WD_t (Water Discharge at time t), RF_t (Rainfall at time t), and AT_t (Average Temperature at time t).

$$\begin{aligned}
 WD_t &= 0.977359 WD_{t-1} \\
 &- 0.101073 WD_{t-2} \quad 1
 \end{aligned}$$

This equation relates the current Water Discharge (WD_t) to its values in the two previous time steps (WD_{t-1} and WD_{t-2}). It implies that the current Water Discharge is influenced by its past values. The positive coefficient (0.977359) on WD_{t-1} suggests a positive auto-

regressive effect, meaning that if the water was discharged in a particular level in the previous time step, it is likely to continue in that level.

Table 4: The Statistical Summary Results for equation AVGTEMP

| | Coefficient | Std. Error | T-Stat | Prob. |
|--------------------|-------------|------------|--------|-------|
| Const. | 6.767784 | 0.963164 | 7.027 | 0.000 |
| L1.WD | 0.001535 | 0.000894 | 1.717 | 0.086 |
| L1.RF | -0.017099 | 0.006230 | -2.745 | 0.006 |
| L1.AVG_TEMP | 0.463519 | 0.028252 | 16.407 | 0.000 |
| L2.WD | -0.001513 | 0.001251 | -1.210 | 0.226 |
| L2.RF | 0.008803 | 0.006788 | 1.297 | 0.195 |
| L2.AVG_TEMP | 0.093533 | 0.033396 | 2.801 | 0.005 |
| L3.WD | 0.000501 | 0.001251 | 0.400 | 0.689 |
| L3.RF | -0.009163 | 0.006774 | -1.353 | 0.176 |
| L3.AVG_TEMP | 0.095567 | 0.033440 | 2.858 | 0.004 |
| L4.WD | 0.000515 | 0.000897 | 0.574 | 0.566 |
| L4.RF | -0.003088 | 0.005943 | -0.520 | 0.603 |
| L4.AVG_TEMP | 0.156961 | 0.028361 | 5.535 | 0.000 |

Table 5: The Correlation matrix of the developed model residuals

| S/No. | WD | RF | AVG_TEMP |
|-----------------|-----------|-----------|-----------|
| WD | 1.000000 | -0.003291 | -0.002285 |
| RF | -0.003291 | 1.000000 | -0.549146 |
| AVG_TEMP | -0.002285 | -0.549146 | 1.000000 |

The negative coefficient (-0.101073) on WD_{t-2} implies a negative auto-regressive effect, indicating that the Water Discharge may have a tendency to change, dampened by the value two-time steps ago.

$$RH_t = 15.357379 + 0.483552RH_{t-1} + 1.146141 AT_{t-1} - 0.436397 AT_{t-2} + 0.161872 RH_{t-3} + 0.100994 RH_{t-4} - 0.581518AT_{t-4} \quad 2$$

This rainfall equation models (Equation 4.4) the current rainfall (RF_t) as a function of several factors. It includes an intercept term of 15.357379, the auto-regressive terms RF_{t-1} , RF_{t-3} , and RF_{t-4} , the lagged effects of average temperature (AT_{t-1} and AT_{t-2}). The equation suggests that current rainfall is influenced by its past values and average temperature in previous time steps. Positive coefficients on the RF terms indicate a positive auto-regressive effect, while negative coefficients on the AT terms imply a dampening effect on rainfall. This equation essentially describes the dynamic relationship between rainfall and these variables.

$$AT_t = 6.767784 - 0.017099 RH_{t-1} + 0.463519 AT_{t-1} + 0.093533 AT_{t-1} + 0.095567 AT_{t-3} - 0.156961 AT_{t-4} \quad 3$$

This equation models the current Average temperature (AT_t) as a function of various factors. It includes an intercept term (6.767784), auto-regressive effects (AT_{t-1} , AT_{t-2} , AT_{t-3} , and AT_{t-4}), and a lagged effect of rainfall (RF_{t-1}). The equation implies that the current Average temperature is influenced by its past values and the previous value of rainfall. The coefficients on these terms indicate how much impact these variables have on the current Average temperature.

The significance of these equations lies in their ability to capture the dynamics and interactions among water discharge, rainfall, and Average temperature. By estimating the coefficients, you can quantify the relationships and predict how changes in these variables at different time

steps will affect one another. These equations can be used in various fields, including meteorology and environmental science, to model and predict weather-related variables.

The Results for Equation WD, Equation 3, provides the coefficients, standard errors, t-statistics, and p-values for the lagged values of the WD variable. The L1. WD has a coefficient of 0.977359, suggesting that the current water discharge (WD) is positively influenced by its previous value.

Also, Results for RF Equation, Equation 4, provides similar information for the Rainfall (RF) variable. It shows how the current RF depends on its own past values and the past values of WD and AVG.TEMP. The L1. RF has a coefficient of 0.483552, indicating that the current RF is positively influenced by its previous value. The Results for AVG. TEMP Equation, Equation 5, provides results for the AVG.

TEMP variable. It shows how the current temperature depends on its past values and the past values of WD and RF. For example, L1.AVG. TEMP has a coefficient of 0.463519, suggesting that the current temperature is positively influenced by its previous value. The model Correlation Matrix of Residuals is given in Table 5: The correlation matrix shows the relationships between the residuals of the equations (errors that are not explained by the model).

A correlation close to -1 or 1 suggests a strong linear relationship between the corresponding residuals. The described modeled graph for the three parameters used for the developed VAR model are shown in Figures 3 to 5

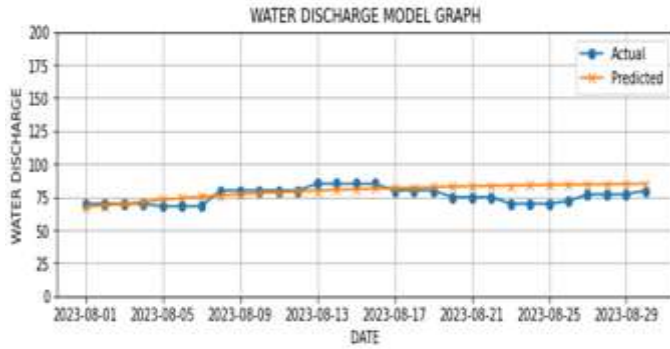


Fig 3: The descript graph of the actual Vs. the predicted graph of the developed

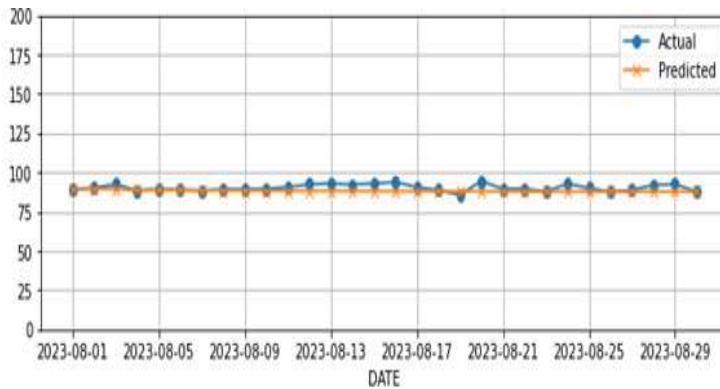


Fig 4: The descript graph of the actual Vs. the predicted graph of the developed

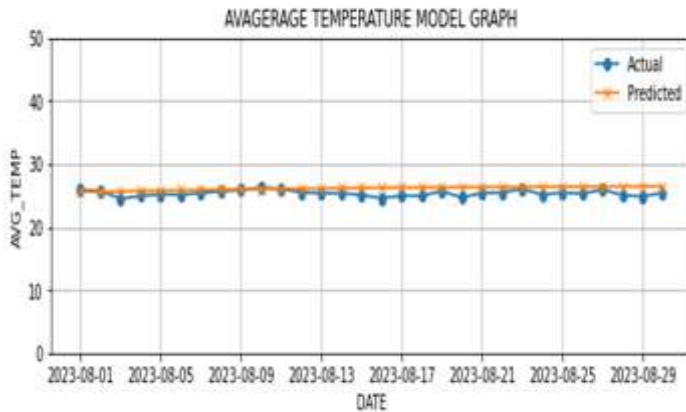


Fig 5: The descriptive graph of the actual Vs. the predicted graph of the developed

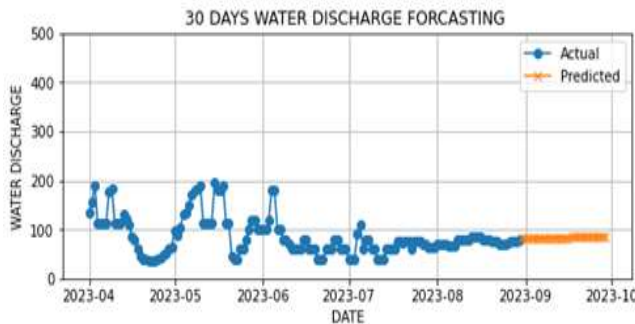


Fig 6: The descriptive graph of the actual Vs. the predicted graph for the next day's forecast for the VAR model

The descriptive graph from Figure 3 to 5 shows that the validation model graph performed very well as it was observed that the predicted line followed in a consistence pattern to the actual data. Though there were little or non-significant deviation from the actual but, generally, made a good model. From Figure 3, the model validation graph for the water discharge shows that the model only over predicted the actual dataset from the 20th to the 28th of August 2023 while the rainfall validation model as shown in Figure 4, under-predicted only on the 15th and the 28th of August 2023, as well as, the Average Temperature validation graph as shown in Figure 5. The Figure 6 shows that the model made a good prediction with R-squared value of 0.9873. This value of R-squared gotten from the forecasted model indicate a very strong correlation with the actual dataset. The performance evaluation measurement results for the developed VAR model is given in Tables 6 to 8 The performance evaluation for the water discharge as shown in Table 6 reveal that *the Mean Absolute Error (MAE)* measures the average absolute difference between the actual values and the predicted values by the VAR model. The significance of a lower MAE indicates that the model's predictions are closer to the actual data points on average. It measures the model's accuracy in terms of the absolute error, regardless of the direction (overestimation or underestimation). The implications of an MAE of 5.5066 means that, on average, the model's predictions for water discharge differ from the actual values by approximately 5.5066 units. *Likewise, the Root Mean Squared Error* is a measure of the square root of the average of the squared differences between the actual and predicted values. The significance: Like MAE, RMSE quantifies the model's accuracy, but it penalizes larger errors more heavily since it involves squaring

the errors. It's a popular choice when giving more weight to larger errors. The implications of an RMSE of 6.7831 means that, on average, the model's predictions for water discharge differ from the actual values by approximately 6.7831 units, with a stronger emphasis on larger errors.

Table 6: The performance evaluation measurement results for the developed Water Discharge VAR model

| S/No. | Evaluation Parameter | Evaluation Measurement |
|-------|---------------------------------------|------------------------|
| 1 | Mean Average Error (MAE) | 5.5066 |
| 2 | Root Mean Square error (RMSE) | 6.7831 |
| 3 | Mean Absolute Percentage Error (MAPE) | 7.4203 |
| 4 | R-Squared (R^2) | 0.8781 |

Table 7: The performance evaluation measurement results for the developed Rainfall VAR model

| S/No. | Evaluation Parameter | Evaluation Measurement |
|-------|---------------------------------------|------------------------|
| 1 | Mean Average Error (MAE) | 2.2178 |
| 2 | Root Mean Square error (RMSE) | 2.9414 |
| 3 | Mean Absolute Percentage Error (MAPE) | 2.4153 |
| 4 | R-Squared (R^2) | 0.9220 |

Table 8: The performance evaluation measurement results for the developed Average Temperature VAR model

| S/No. | Evaluation Parameter | Evaluation Measurement |
|-------|---------------------------------------|------------------------|
| 1 | Mean Average Error (MAE) | 0.8204 |
| 2 | Root Mean Square error (RMSE) | 0.9392 |
| 3 | Mean Absolute Percentage Error (MAPE) | 3.2626 |
| 4 | R-Squared (R^2) | 0.9017 |

Also, the Mean Absolute Percentage Error (MAPE) measures the average percentage difference between the actual values and the predicted values, making it a relative error metric. The significance of MAPE is useful for understanding the model's accuracy in terms of percentage errors. It's especially informative when to assess the model's performance relative to the scale of the data. From Table 6, the implications of a MAPE of 7.4203% means that, on average, the model's predictions for water discharge differ from the actual values by approximately 7.4203% in terms of relative error. However, the R-squared, also known as the coefficient of determination, measures the proportion of the variance in the dependent variable (water discharge in this case) that is explained by the independent variables (the VAR model predictions) provides insights into how well the model fits the data. An R^2 value of 0.8781 which is close to +1 suggests that the model explains a substantial portion of the variance in the data. It indicates that approximately 87.81% of the variability in water discharge can be accounted for by the VAR model, which suggests that the model is providing a good fit to the data. Generally, these validation metrics help assess the accuracy, precision, and goodness of fit of your VAR model for water discharge. A low MAE, RMSE, and MAPE indicate good prediction accuracy, while a high R-squared suggests that the model is a good fit for the data. These metrics collectively provide a comprehensive evaluation of the model's performance and can help determine its utility in making forecasts or predictions.

Conclusion: The study employed Vector Autoregressive models (VAR) for rainfall-riverflow modeling of Enyong Creek, Akwa Ibom State, Nigeria. The model effectively captured the dynamic relationships between water discharge, rainfall, and average temperature,

demonstrating its potential for flood forecasting in the region. It improves early warning systems for proactive disaster preparedness and management with emphasizes on the importance of incorporating advanced modeling techniques for disaster risk reduction.

REFERENCES

- Ahaneku, IE; Otache, MY (2014). Stochastic characteristics and modelling of monthly rainfall time series of Illorin, Nigeria. *Open J. of Modern Hydrology* 4(3) :67-79
- Alfieri, L; Pappenberger, F (2019). Climate change and early warning systems for river floods. In *Handbook of Hydrometeorology* (pp. 1-32). Springer, Cham.
- Borga, M; West, J; Bell, JD; Harvey, NC; Romu, T; Heymsfield, SB; Dahlqvist, LO (2014). Advanced body composition assessment: from body mass index to body composition profiling. *J. Magnetic Resonance Imaging*, 40(6), 1437-1444. Box, GEP; Jenkins, GM; Reinsel, GC (1994). *Time series analysis forecasting and control* (Vol. 34). Prentice Hall, Upper Saddle River, NJ.
- Brockwell, PJ; Davis, RA (2009). *Time series: Theory and methods* (2nd ed.). Springer.
- Chang, YH; Guo, JY (2006). A novel approach for predicting stock market trend: Hybrid model based on particle swarm optimization and support vector machine. In *2006 IEEE International Conference on Machine Learning and Cybernetics* (Pp. 2689-2693). IEEE.

- Dinh, JE; Lord, RG; Gardner, WL; Meuser, JD; Liden, RC; Hu, J(2014). Leadership theory and research in the new millennium: Current theoretical trends and changing perspectives. *The Leadership Quarterly*, 25(1), 36-62.
- Helmut L. (2007). Econometric Analysis with Vector Autoregressive Models. *International Encyclopedia of Statistical Science*. DOI:10.1002/9780470748916.CH8 Corpus ID: 124310420
- Hyndman, RJ; Athanasopoulos, G (2018). Forecasting: methods and applications (Vol. 80). Springer, Cham.
- Jonkman, SN; Dawson, RJ (2012). Issues and challenges in flood risk management: *Editorial for the special issue on flood risk management*. *Water*, 4(4), 785-792.
- Khan, SI; Hong Y; Wang, J; Yilmaz, KK; Gourley, JJ; Irwin, D (2011). Satellite remote sensing and hydrologic modeling for flood inundation mapping in Lake Victoria basin: Implications for hydrologic prediction in ungagged basins. *IEEE Transportation Geosci. Remote Sensing*. **49**, 85–95.
- Kidd, C; Huffman, GJ (2011). Global precipitation measurement: A story of progress, challenges, and unmet needs. In *Measuring Precipitation from Space: Evolving Technologies and Applications* (Pp. 1-34). Springer, Dordrecht.
- Linsley, RK; Kohler, MA; Paulhus, JLS (1975). *Hydrology for Engineers*. (3rd ed.). McGraw-Hill Book Company.
- Merz, B; Kreibich, H; Apel, H; Vorogushchin, S; Dottori, M; Disse, M (2020). Impact forecasting to support emergency management of natural hazards. *Rev. Geophy.* 58(1), e2019RG000748.
- Parker, DJ; Wilby, RL (2005). Flood Forecasting: A Review of Methods, Challenges, and Approaches. *J. Prog. Phys. Geog.* 29(4), 311-323. DOI: 10.1191/030502405pp471pr
- World Meteorological Organization (WMO), (2023). Flood Forecasting Initiative. <https://community.wmo.int/en/activity-areas/world-meteorological-organization-flood-forecasting-initiative>